Available online at www.sciencedirect.com
SCIENCE DIRECT®
Biomaterials 27 (2006) 1924–1929
Biomaterials
www.elsevier.com/locate/biomaterials

Technical Note

# A method for solvent-free fabrication of porous polymer using solid-state foaming and ultrasound for tissue engineering applications

Xiaoxi Wang, Wei Li*, Vipin Kumar

*Department of Mechanical Engineering, University of Washington, Seattle, WA 98195-2600, USA*

Received 10 May 2005; accepted 26 September 2005
Available online 10 October 2005

**Abstract**

Most of the existing fabrication techniques for tissue engineering scaffolds require the use of organic solvents that may never be fully removed even after long leaching hours. The residues of these organic solvents reduce the ability of biological cells to form new tissue. This paper presents an approach toward solvent-free fabrication of tissue engineering scaffolds. Interconnected porous structures were created using solid-state foaming and ultrasound. The material used in this study was polylactic acid (PLA) and the blowing agent was $CO_2$. In order to determine suitable process conditions, saturation and foaming studies were first conducted. Selected foam samples were then processed using pulsed ultrasound. The microstructures before and after the ultrasound processing were compared. It was shown that the inter-pore connectivity of the solid-state foams was substantially enhanced. The combined solid-state foaming and ultrasound processing provide a way to fabricate porous polymer for potential tissue engineering applications.


*Keywords:* Solvent-free fabrication; Tissue engineering scaffold; Polylactic acid (PLA); Ultrasound; Solid-state foams; Porous polymer

## 1. Introduction

Over the past decade, tissue engineering has moved beyond the realm of transplantation and into the realm of fabrication [1]. The vision is that in the future doctors will be able to shape the scaffolds into intricate structures that mimic specific tissue and organs, load the scaffolds with living cells and nutrient, and implant them to replace diseased or damaged organs without the need of retrieving the scaffolds. For this to be successful, the fabrication of biodegradable tissue engineering scaffolds is crucial. Existing fabrication methods for tissue engineering scaffolds include the fiber bonding [2], solvent casting [3–5], phase separation [6–11], gas foaming with particulate leaching [12–16], and rapid prototyping techniques [17–19]. Almost all these methods require organic solvents, which may reduce the ability for biological cells to form new tissue if not fully removed. Other methods involve using salt particulates as porogen. The concerns for this are the lengthy leaching steps and the residual salt effects. To overcome these problems, other combinations of materials and pore-forming techniques must be explored [2].

The solid-state foaming process has been studied to generate microcellular foams for biomedical applications [20]. The process does not involve any organic solvents or chemical blowing agents. Instead, it uses gases such as $CO_2$ and $N_2$. The pore sizes that have been achieved range from sub-micrometers to a few hundred micrometers. However, the disadvantage of the process is that the foams it produces are mostly close-pored and not suitable for tissue engineering applications. In this study, we explore the possibility of using ultrasound to break the pore walls of the solid state foams. Biodegradable polymer samples were first foamed in the solid-state foaming process to achieve suitable pore sizes. Then the foamed samples were processed using ultrasound. The microstructures of the processed samples were compared with those of the original foams. It is shown that ultrasound can substantially enhance the inter-pore connectivity of the solid-state foams, which suggests that the combined solid-state foaming and ultrasound process could be used to fabricate biodegradable porous polymer for tissue engineering applications.

*Corresponding author. Tel.: +1 (206) 543-5339.
*E-mail address:* weiwli@u.washington.edu (W. Li).

0142-9612/$ - see front matter © 2005 Elsevier Ltd. All rights reserved.
doi:10.1016/j.biomaterials.2005.09.029

## 2. Experimental

### 2.1. Materials

Biodegradable polylactic acid (PLA) was used in the study. The PLA samples were acquired in thin sheets (0.25 mm) (WMI, Taiwan) and compression molded into thicker samples (1.1–1.3 mm). The density of the samples was 1.25 g/cm$^3$. PLA is a semicrystalline polymer. The crystallitnity of the samples after the compression molding was around 5%. The glass transition temperature was 60 °C. Medical grade $CO_2$ was used as the physical blowing agent. The $CO_2$ was obtained from Airgas Nor Pac, Inc.

### 2.2. Experimental setup and procedure

The PLA samples were foamed in a typical solid-state foaming process [20]. Before foaming a PLA–$CO_2$ sorption study was conducted at room temperature with the gas pressures at 3–5 MPa. Following the sorption study at 5 MPa, a desorption study was conducted by retrieving a sample from the pressure vessel and measuring its weight periodically in the atmospheric environment. The results of these sorption and desorption studies were used to determine the saturation time and desorption time, both of which are important for the subsequent foaming process.

The foaming experiments were conducted in two groups. In the first group, the saturation time and desorption time were kept constant, while the major process parameters including saturation pressure, foaming temperature, and foaming time were varied according to Table 1. Desorption time was defined as the time elapse between when the samples were retrieved from the pressure vessel to when they were foamed. The purpose of this group of experiments was to identify the relationship between the pore size and the major foaming process parameters. In the second group of experiments, the effects of the saturation time and desorption time were explored. Table 2 shows the parameters used in the second group of the experiments.

After foaming, the relative density of the samples was measured according to ASTM standard [21]. Foamed samples with the lowest relative density were chosen to apply ultrasound (Model VC750 from Sonics Concept, Inc.). The ultrasonic processor had a frequency of 20 kHz and a maximum power of 750 W. The samples were held with a fixture in distilled water. The water container was located on a positioning table that was computer controlled (MAXNC 10 from MAXNC, Inc.). The sonotrode was placed 2 mm above the sample surface. Pulsed ultrasound was used with a 1:9 on and off ratio and the average electrical power was maintained at 100 w. The total ultrasound treatment time was 60 s. The water temperature was 21 °C.

### 2.3. Sample characterization

FEI Siron XL 30 EDAX EDS scanning electronic microscope (SEM) was used for microstructure characterization. Image processing software, *ImageJ*, from the NIH website was used to analyze the pore size distribution. The pore size was measured from the SEM images as the Feret's diameter, i.e., the greatest distance possible between any two points along the boundary of the pore.

Table 1
Parameters in the first group foaming experiments

| Variable | Values |
|---|---|
| Saturation pressure (MPa) | 3, 4, 5 |
| Saturation time (h) | 165 |
| Desorption time (min) | 60 |
| Foaming temperature (°C) | 100, 130, 140, 150 |
| Foaming time (s) | 5, 20, 60 |

Table 2
Parameters in the second group foaming experiments

| Variable | Values |
|---|---|
| Saturation pressure (MPa) | 5 |
| Saturation time (h) | 3.5, 30 |
| Desorption time (min) | 10–50 |
| Foaming temperature (°C) | 100 |
| Foaming time (s) | 10 |

## 3. Results and discussion

### 3.1. $CO_2$ saturation and desorption of PLA

The $CO_2$ saturation results of PLA samples are shown in Fig. 1. The equilibrium $CO_2$ concentration in the polymer samples was 11%, 15% and 21% for saturation pressures of 3, 4, and 5 MPa, respectively. Despite the difference in saturation pressures, all the samples reached the equilibrium in less than 20 h. The saturation results suggest that the solid-state foams can be produced in a relatively short time frame. Fig. 2 shows the results from the saturation and desorption studies with a sample saturated at 5 MPa. It is seen that the gas concentration started to decrease at a faster rate once it was taken out the pressure vessel. Within six hours, the gas concentration decreased from 20% to about 8%. This indicates that the desorption time could be a significant factor affecting the foaming process. Samples foamed at different desorption times could have different relative density since the gas concentration of the saturated samples could be dramatically different. Therefore, desorption time should be carefully controlled to obtain consistent foaming results.

### 3.2. The effects of foaming parameters

A statistical analysis was conducted on the main effects and the second order interaction effects of the three major foaming process parameters. Table 3 shows the results of an *F*-test using the standard least squares regression algorithm. Based on the *F*-test results, it can be determined that the main effects of the saturation pressure and foaming temperature have significant effects on the relative foam density. The main effect of the foaming time is insignificant. However, the interaction effect of the foaming temperature and foaming time is significant.

The main effects of these three parameters are plotted in Fig. 3. In general, foaming temperature has the most significant effect on the relative density. The higher the foaming temperature is, the lower the relative density will be. As the saturation pressure increases, the relative density decreases. When the foaming time increases, the relative density also increases. The interaction effects of these three parameters are plotted in Fig. 4. The interaction of the foaming temperature and time shows strong effect, which means they have to be considered jointly to achieve a low

relative density. When the foaming temperature is 100 °C, the relative density reduces as the foaming time increases. On the other hand, when the foaming temperature is 150 °C the relative density increases with the foaming time.

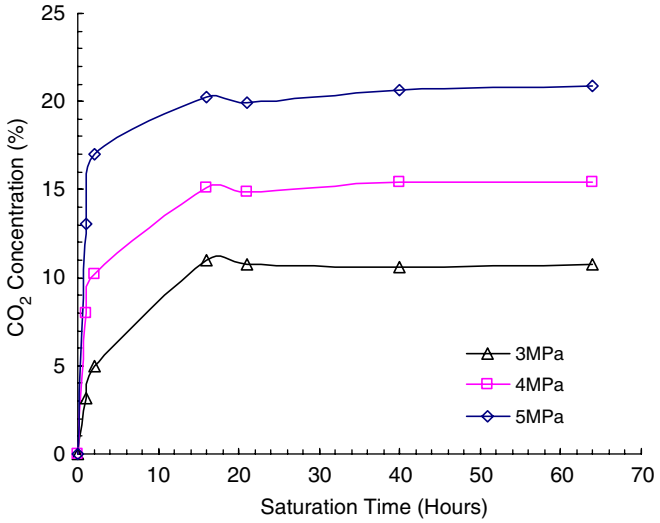


Fig. 1. $CO_2$ uptake at room temperature, expressed as weight percent of PLA samples as a function of saturation pressure and time. The sample thickness was 1 mm.

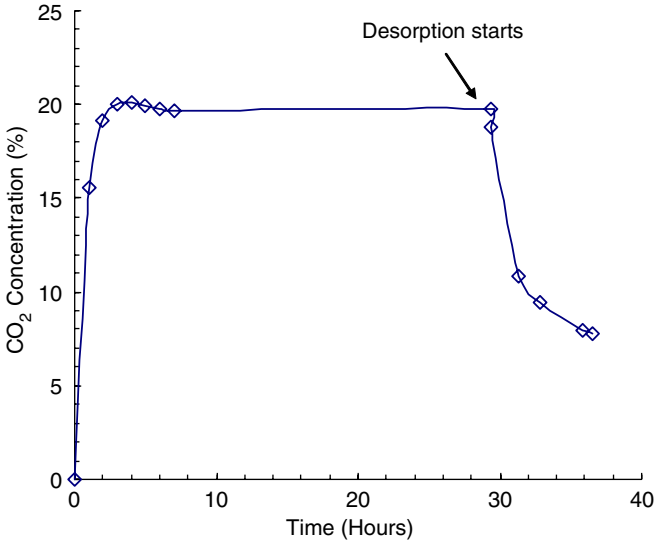


Fig. 2. Saturation and desorption study at room temperature with a saturation pressure of 5 MPa.

The effect of saturation time is shown in Fig. 5(a). On average, the samples saturated for 3.5 h have a lower relative density than those saturated for 30 h. This is because that after 20 h of saturation the PLA sample is believed to enter an annealing state where a higher fraction of the polymer becomes crystallized. High crystallinity content in the PLA samples prevents the formation of low-density foams. The effect of desorption time is shown in Fig. 5(b). Within the first 15 min of desorption time, the relative density reduces significantly. After that the relative density becomes stable. The reason is that with a short desorption time the gas concentration at the surface layers of the samples is still high. It will foam and provide passages for the gas deep inside to escape without participating in the foaming process. Therefore, a certain amount of desorption time is needed to create low density foams. On the other hand, the desorption time cannot be too long as the gas will simply diffuse away in that case. Although the relative density varies with the desorption time, it can be seen that there is a relatively wide processing window of 15–45 min where the relative density stays consistently low. This window is long enough for retrieving the samples from the pressure vessel and completing the foaming process.

### 3.3. The effect of ultrasound treatment

The ultrasound treatment was applied to foamed samples with the lowest relative density (9% in this case). These samples were saturated at 5 MPa for 3.5 h. The desorption time was 40 min. The foaming temperature was 100 °C and the foaming time was 10 s. The microstructures of a sample before and after the ultrasound exposure are shown in Fig. 6. Before the ultrasound application, most pores were closed. After the ultrasound exposure, the pores became mostly open. To examine the effect of the ultrasound on the pore size, the pore size distributions before and after the ultrasound treatment are compared in Fig. 7. Before the ultrasound treatment, the diameters of the closed pores varied from 30 to 70 μm. After the ultrasound treatment, the interconnected pore sizes changed to 30–90 μm. As shown, the overall pore size distribution shifted slightly to the right, which indicated that the average pore size becomes only a little bigger after the ultrasound treatment.

Table 3
The significance of the foaming parameters

| Source | DF | Sum of squares | $F$ ratio | Prob > $F$ |
|---|---|---|---|---|
| Saturation pressure | 1 | 0.2395 | 12.857 | 0.0037 |
| Foaming temperature | 1 | 0.2246 | 12.057 | 0.0046 |
| Foaming time | 1 | 0.0152 | 0.8184 | 0.3835 |
| Saturation pressure × foaming temperature | 1 | 0.0000 | 0.0021 | 0.9640 |
| Saturation pressure × foaming time | 1 | 0.0008 | 0.0404 | 0.8440 |
| Foaming temperature × foaming time | 1 | 0.15586 | 8.3651 | 0.0135 |

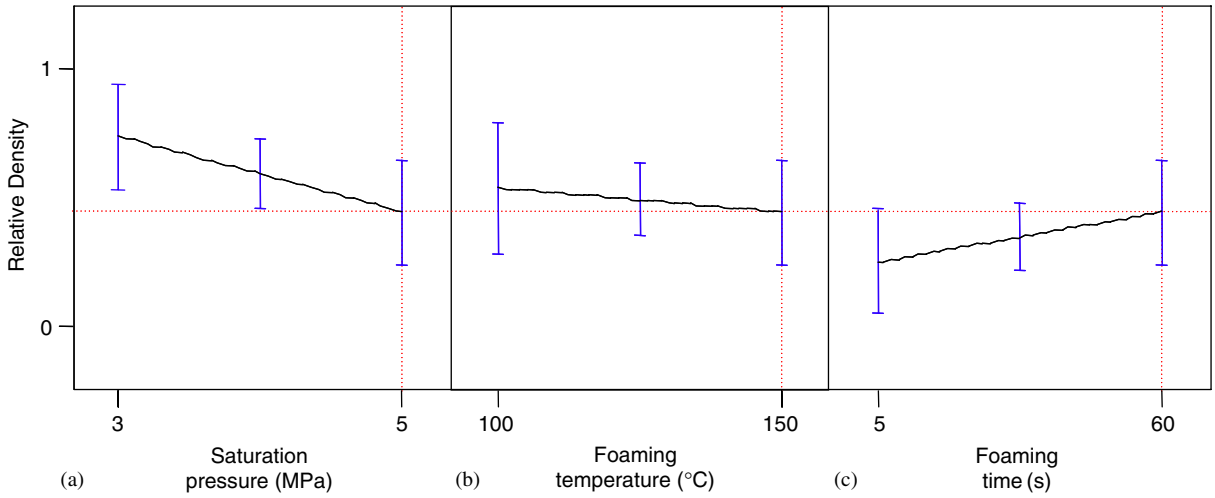


Fig. 3. Effects of (a) saturation pressure, (b) foaming temperature, and (c) foaming time on the relative density.

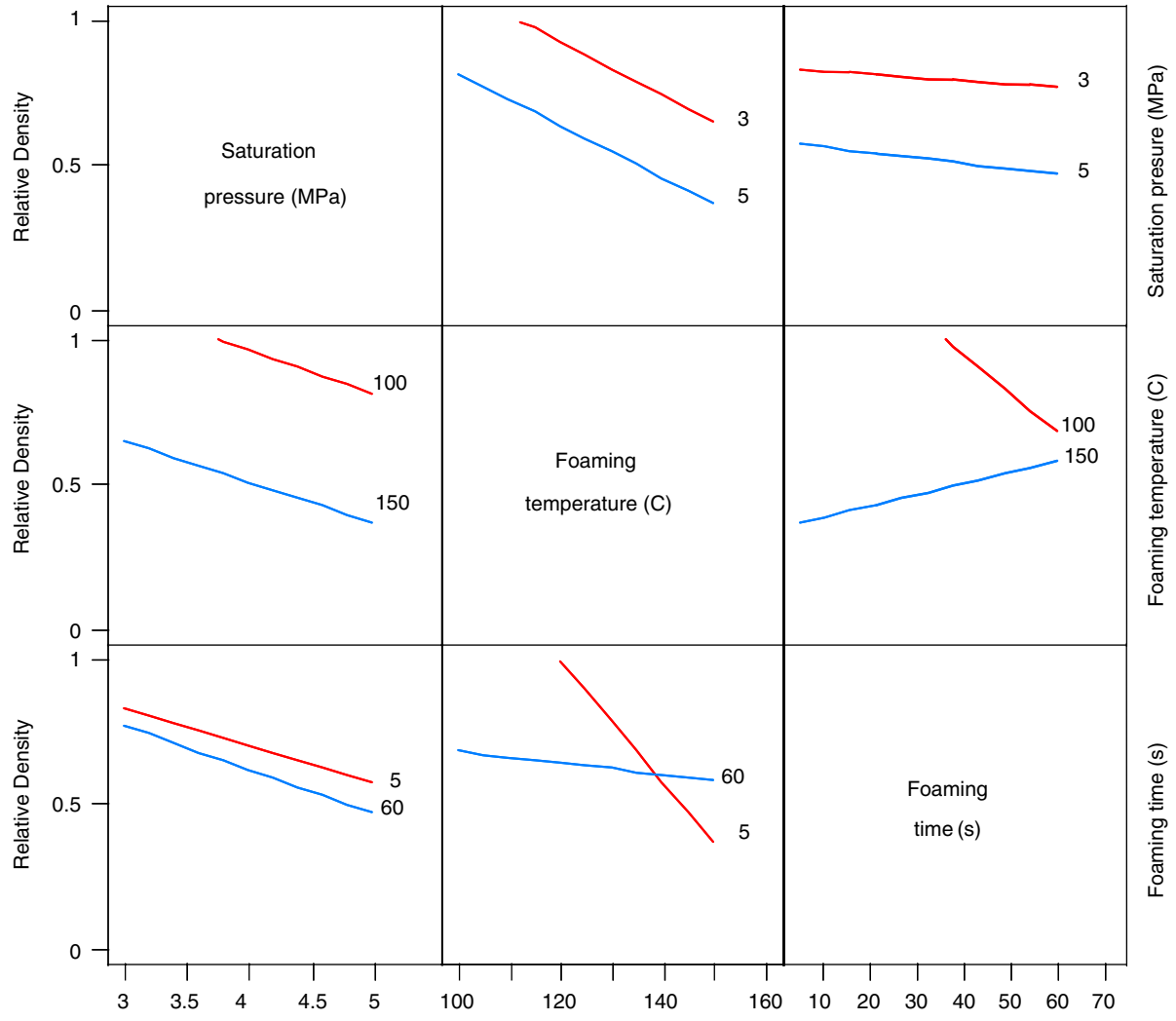


Fig. 4. Interaction plots of the three process variables, showing a strong interaction effect between foaming temperature and foaming time.

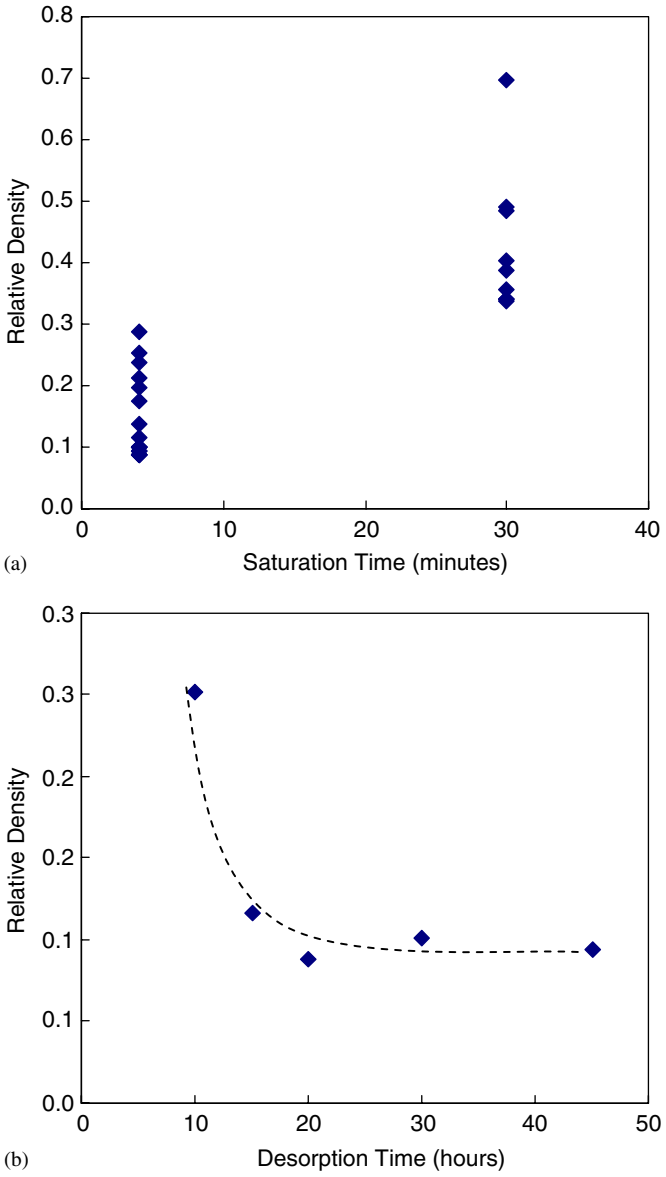


Fig. 5. Effects of saturation time and desorption time: (a) relative density increases with saturation time at 5 MPa and (b) relative density decreases with desorption time. Note these results are only true within certain limited ranges.

Interconnected pores in the foam are the result of pore wall rupture. When gas saturated polymer is foamed in the solid-state foaming process, gas bubbles will nucleate and grow to form the pores. When they grow large enough, the bubbles will impinge on one another and could rupture owing to the stretching from other regions of the foam. Bubble rupture in the solid-state foaming process is undesirable. As soon as most of the bubbles rupture, the foam will collapse and become solid again since the polymer is still soft at the foaming temperature. In this study, the foam bubbles were allowed to grow to their maximum sizes. Ultrasound was applied after the samples have cooled down. Being a pressure wave, ultrasound can be transmitted through any substance that possesses elastic

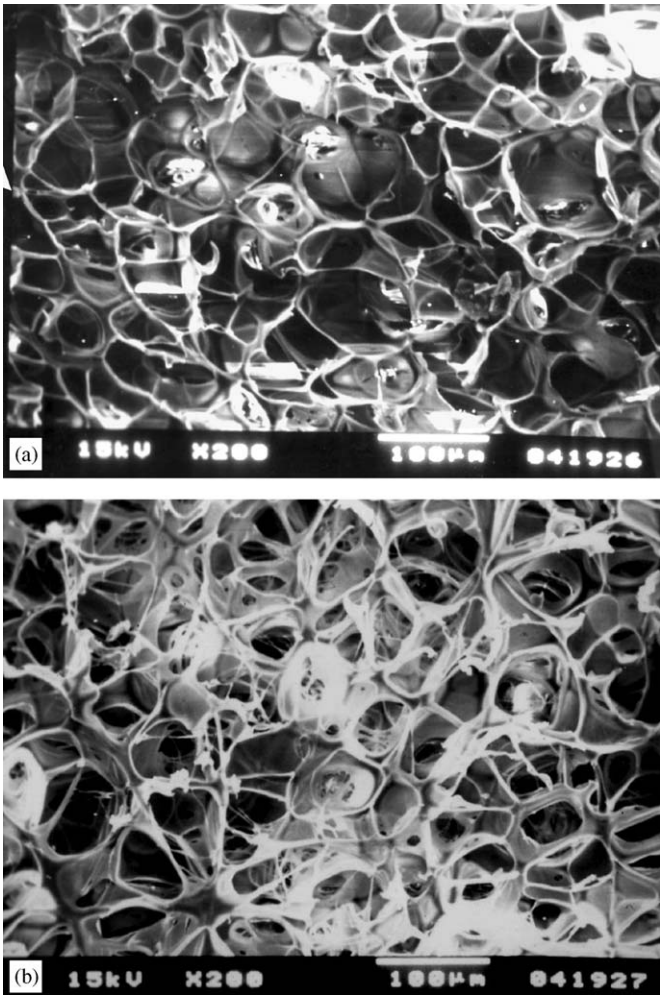


Fig. 6. The effect of ultrasound: (a) PLA foam before ultrasound exposure and (b) after ultrasound exposure, showing a porous structure with enhanced inter-pore connectivity.

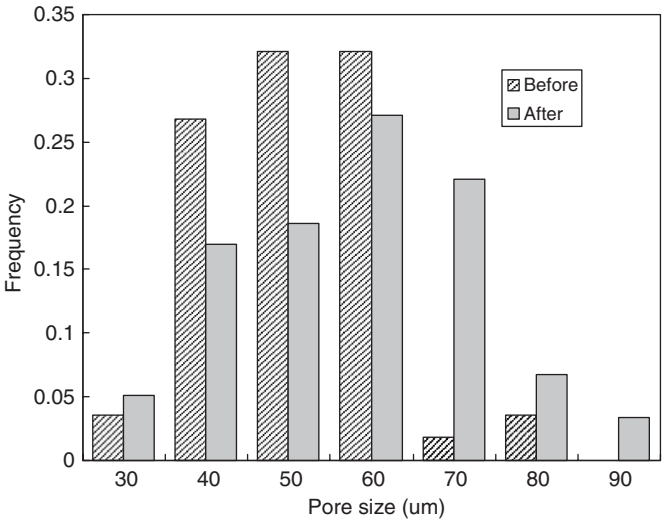


Fig. 7. Pore size distributions before and after the ultrasound exposure, showing the bubble size was not significantly affected by ultrasound.

properties. When the ultrasound intensity is high enough, the substance could be "torn apart" microscopically during the tension cycle. In addition, ultrasound has a heating effect inside the polymer foam. The heat generated in the foam could add expansion to the thin bubble walls, helping them to break. Since the heat generation is local and the overall temperature is still low, the foam will have enough strength to maintain its overall shape without collapsing as a whole.

## 4. Conclusions

This paper presented a solvent-free fabrication method for biodegradable porous polymer. Ultrasound was applied after the solid state foaming process to create interconnected porous structures. It has been found that biodegradable PLA can be foamed using the solid-state foaming process with a wide processing window and the inter-pore connectivity of the foams was substantially enhanced by applying ultrasound treatment. The combined solid-state foaming and ultrasound processing method could provide a completely solvent-free approach to fabricating porous polymer for tissue engineering applications.

## Acknowledgments

This work was partially supported by the US National Science Foundation, award No. DMI-0300415.

## References

[1] Chaignaud BE, Langer R, Vacanti JP. The history of tissue engineering using synthetic biodegradable polymer scaffolds and cells. In: Atala A, Mooney D, editors. Synthetic biodegradable polymer scaffolds. 1997. p. 1–4.
[2] Mikos AG, Temenoff JS. Formation of highly porous biodegradable scaffolds for tissue engineering. J Biotechnol 2000;2:114–9.
[3] Mikos AG, Bao Y, Cima LG, Ingber DE, Vacanti JP, Langer R. Preparation of poly(glycolic acid) bonded fiber structures for cell attachment and transplantation. J Biomed Mater Res 1993;27:183–9.
[4] Mikos AG, Thorsen AI, Czerwonka LA, Bao Y, Langer R, Winslow DN, Vacanti IP. Preparation and characterization of poly(L-lactic acid) foams. Polymer 1994;35:1068–77.
[5] Shastri VP, Martin I, Langer R. Macroporous polymer foams by hydrocarbon templating. Proc Natl Acad Sci USA 2000;97:1970–5.
[6] Whang K, Thomas CH, Healy KE, Nuber G. A novel method to fabricate bioabsorbable scaffolds. Polymer 1995;36:837–42.
[7] Lo H, Kadiyala S, Guggino SE, Leong KW. Poly(L-lactic acid) foams with cell seeding and controlled-release capacity. J Biomed Mater Res 1996;30:475–84.
[8] Lo H, Ponticiello MS, Leong KW. Fabrication of controlled release biodegradable foams by phase separation. Tissue Eng 1995;1:15–28.
[9] Schugens C, Maquet V, Grandfils C, Jerome R, Teyssie P. Polylactide macroporous biodegradable implants for cell transplantation II: preparation of polylactide foams for liquid–liquid phase separation. J Biomed Mater Res 1996;30:449–61.
[10] Nam YS, Park TG. Biodegradable polymeric microcellular foams by modified thermally induced phase separation method. Biomaterials 1999;20:1783–90.
[11] Nam YS, Park TG. Porous biodegradable polymeric scaffolds prepared by thermally induced phase separation. J Biomed Mater Res 1999;47:8–17.
[12] Mooney DJ, Baldwin DF, Suh NP, Vacanti JP, Langer R. Novel approach to fabricate porous sponges of poly(D,L-lactic-*co*-glycolic acid) without the use of organic solvents. Biomaterials 1996;17:1417–22.
[13] Park TG. New approaches to fabricate highly porous tissue scaffolds. The Fourth Asia-Pacific conference on medical and biological engineering, Seoul, Korea, 1999.
[14] Nam YS, Yoon JJ, Park TG. A novel fabrication method of macroporous biodegradable polymer scaffolds using gas foaming and salt as a porogen additive. J Biomed Mater Res: Appl Biomater 2000;53:1–7.
[15] Sparacio D, Beckman EJ. Generation of microcellular biodegradable polymers in supercritical carbon dioxide. Polymer Preprints: Division of Polymer Chemistry, American Chemical Society, vol. 38(2), 1997. p. 420–3.
[16] Harris LD, Kim BS, Mooney DJ. Open pore biodegradable matrices formed with gas foaming. J Biomed Mater Res 1998;42:396–402.
[17] Park A, Wu B, Griffith LG. Integration of surface modification and 3D fabrication techniques to prepare patterned poly(L-lactide) substrates allowing regionally selective cell adhesion. J Biomater Sci Polym Ed 1998;9:89–110.
[18] Landers R, Mülhaupt R. Desktop manufacturing of complex objects, prototypes and biomedical scaffolds by means of computer-assisted design combined with computer-guided 3D plotting of polymers and reactive oligomers. Macromol Mater Eng 2000;282:17–21.
[19] Ang TH, Sultana FSA, Hutmacher DW, Wong YS, Fuh YH, Mob HT, et al. Fabrication of 3D chitosan-hydroxyapatite scaffolds using a robotic dispensing system. Mater Sci Eng: C 2002;20(1–2):35–42.
[20] Singh L, Kumar V, Ratner BD. Generation of porous microcellular 85/15 poly(D,L-lactide-*co*-glycolide) foams for biomedical applications. Biomaterials 2004;25(13):2611–7.
[21] ASTM D-792. Standard test methods for density and specific gravity (relative density) of plastics by displacement. West Conshohocken, PA: ASTM International; 2002.